Reversing and non-reversing modulated Taylor–Couette flow

By ANTHONY J. YOUD, ASHLEY P. WILLIS
AND CARLO F. BARENGHI

Department of Mathematics, University of Newcastle, Newcastle upon Tyne, NE1 7RU, UK

We study time-modulated Taylor–Couette flow for the simple case in which the inner cylinder's angular velocity oscillates around zero mean at given amplitude and frequency and the outer cylinder is at rest. We find that, provided the amplitude of modulation is large enough, two classes of Taylor vortex flows are possible – reversing and non-reversing. In the latter, which takes place at relatively high frequency, the direction of the Taylor vortices does not change every half-cycle.

1. Introduction

The classical formulation of the Taylor–Couette flow problem consists of an incompressible fluid of constant density and viscosity which is contained between two coaxial cylinders. Typically the height of the cylinders is much larger than the gap between them, the outer cylinder is held fixed, and the inner cylinder is kept in rotation at constant angular velocity Ω_1. If Ω_1 is small, the velocity field is purely azimuthal (circular Couette flow), but if Ω_1 exceeds a critical value Ω_{10}, then axisymmetric perturbations become unstable and the resulting secondary flow consists of alternating pairs of vortices in the axial direction (Taylor vortex flow). At higher velocity Taylor vortex flow loses stability to non-axisymmetric perturbations (wavy modes). If the drive is increased, further transitions take place, and, if one allows rotations of the outer cylinder, the variety of flows is even richer.

Our concern is the case in which Ω_1 is not constant but oscillates harmonically in time. This modulated Taylor–Couette problem has been the subject of a number of investigations which attempted to answer the natural question of whether the modulation makes the flow more or less stable to the onset of vortices than in the steady case. The problem can also be tackled in the context of spherical Couette flow, as recently done by Zhang (2002) and Zhang & Zhang (2002). The oscillating boundary induces a damped viscous wave which penetrates into the fluid a distance of the order of the thickness of the Stokes layer, $\delta_s = (2\nu/\omega)^{1/2}$, where ν is the kinematic viscosity and ω is the frequency of modulation. In this paper we are concerned with the basic case in which the frequency is low enough that the size of the Stokes layer is comparable to the gap between the cylinders. The high-frequency limit of a thin Stokes layer, which was studied for example by Barenghi, Park & Donnelly (1980) in cylindrical geometry and by Hollerbach *et al.* (2002) in spherical Couette flow, will not be addressed here.

The most studied case of modulated Couette flow is that in which the inner cylinder oscillates about some mean value with some given amplitude

$$\Omega_1(t) = \Omega_{1m} + \Omega_{1a} \cos(\omega t), \tag{1.1}$$

such that the peak angular velocity $\Omega_{1m} + \Omega_{1a}$ is of the order of the onset of vortices in the steady case, Ω_{10}. In particular we note the experiments of Donnelly (1964) and Walsh & Donnelly (1988a, b), who discovered that at low frequency of modulation the stability of the flow is greatly enhanced. On the theoretical side, the problem was tackled in the narrow gap limit by Hall (1983), who derived an amplitude equation, and by Riley & Lawrence (1977), who used Floquet theory. Carmi & Tustaniwskyj (1981) extended the Floquet approach to finite values of radius ratio. Barenghi & Jones (1989) and Barenghi (1991) solved the Floquet problem as well as the fully nonlinear time-dependent Navier–Stokes equation, and compared their finite-amplitude, time-dependent solutions to measurements. A similar approach was followed by Kuhlmann, Roth, & Luecke (1989), who also developed a mode truncation model. Mode truncation was also used by Hsieh & Chen (1984) and Bhattacharjee, Banerjee & Kumar (1986). Almost all of these authors did not limit themselves to the most studied case (equation (1.1) with $\Omega_{1m} + \Omega_{1a} \approx \Omega_{10}$), but studied other variations of the problem, including steady and periodic motions of the outer cylinder. More recently a new class of time-modulated Taylor–Couette problems in which the inner cylinder moves periodically in the axial direction has been introduced and studied by Marques & Lopez (1997) and Lopez & Marques (2001).

Since the parameter space of the modulated Taylor–Couette problem is so large (besides the radius ratio, one has to specify mean value, amplitude and frequency of modulation of each cylinder), there are many interesting cases to study. The aim of this paper is to present a new class of solutions of the simplest of all cases, that in which the outer cylinder is fixed and the inner cylinder oscillates around zero mean, like a washing machine:

$$\Omega_1(t) = \Omega_{1a} \cos(\omega t). \tag{1.2}$$

2. Formulation of the problem

We use cylindrical coordinates (r, ϕ, z), call R_1 and R_2 respectively the inner and outer radius and make the usual assumption that the cylinders have infinite height. The flow is described by the incompressible Navier–Stokes equations

$$\frac{\partial \boldsymbol{v}}{\partial t} + \boldsymbol{v} \cdot \nabla \boldsymbol{v} = -\frac{1}{\rho} \nabla p + \nu \nabla^2 \boldsymbol{v}, \tag{2.1}$$

$$\nabla \cdot \boldsymbol{v} = 0, \tag{2.2}$$

where $\boldsymbol{v}$ is the velocity and p is the pressure. The density, ρ, and the kinematic viscosity, ν, are constant. The boundary conditions for $\boldsymbol{v}$ are the no-slip conditions, so $v_r = v_\phi = v_z = 0$ at $r = R_2$, and $v_r = v_z = 0$, $v_\phi = R_1 \Omega_1(t)$ at $r = R_1$, where $\Omega_1(t)$ is given by equation (1.2). We make the equations dimensionless using the length scale $\delta = R_2 - R_1$ and the viscous time scale δ^2/ν. Equation (1.2) is then expressed in terms of the Reynolds number

$$Re_1(t) = Re_{mod} \cos(\omega t), \tag{2.3}$$

where $Re_{mod} = \Omega_{1a} R_1 \delta / \nu$ and now t and ω are the dimensionless time and frequency of modulation respectively. The other parameter of the problem is the radius ratio $\eta = R_1/R_2$. We call $Re_{10} = \Omega_{10} R_1 \delta / \nu$ the Reynolds number which corresponds to the onset of Taylor vortex flow in the steady case.

Equations (2.1) and (2.2) are time stepped using a combination of second-order-accurate Crank–Nicolson and Adams–Bashforth methods. The velocity components are represented by potentials which are expanded spectrally over Fourier modes in

the azimuthal and axial directions and over Chebyshev polynomials in the radial direction, for which a generic field $A(x, \phi, z, t)$ has the form

$$A(x, \phi, z, t) = \sum_{n=0}^{N} \sum_{|k|<K} \sum_{|m|<M} A_{nkm}(t) \, T_n^*(x) \mathrm{e}^{\mathrm{i}(\alpha k z + m\phi)} \tag{2.4}$$

on the domain $[0, 1] \times [0, 2\pi] \times [0, 2\pi/\alpha]$ where $T_n^*(x)$ is the nth shifted Chebyshev polynomial and x is given by $r = \eta/(1 - \eta) + x$. Spectral truncations as high as $K = 12$, $M = 8$ and $N = 16$ were used, where K, M and N are the numbers of axial, azimuthal and radial modes respectively.

The details have been published in Willis & Barenghi (2002). Here it suffices to say that the code has been tested in the linear and nonlinear axisymmetric regime against published results of Barenghi (1991) and Jones (1985). Tests of the code in the wavy mode regime have been done against the findings of King *et al.* (1984) and Marcus (1984).

3. Results

All our calculations are performed at radius ratio $\eta = 0.75$. At this value of η, in the steady case, the critical Reynolds number for the onset of Taylor vortex flow is $Re_{10} = 85.78$ and the (dimensionless) critical axial wavenumber is $\alpha_c = 3.13$. In the modulated case α depends strongly on the frequency of modulation ω. The calculations that follow were performed with variable α to determine the critical axial wavenumber at each frequency. We have also performed fully three-dimensional calculations that allow the existence of non-axisymmetric wavy modes, but found that, within the parameter range explored, the wavy modes always decay and the resulting solution is axisymmetric. Our initial conditions consist of seeding all the spectral modes for the velocity components with small random numbers of order of magnitude 10^{-3}; we then integrate the equations of motion in time, until, after an initial transient, a settled oscillation is achieved.

3.1. *Reversing Taylor vortex flow*

Typical results at small frequency of modulation ($\omega \lesssim 4$) are shown in figure 1. The solid curve represents the radial velocity component $v_r(t)$ computed at the outflow jet ($z = \pi/\alpha$) in the middle of the gap. Since v_r vanishes when the flow is purely azimuthal (circular Couette flow), by monitoring its value we detect the existence of Taylor vortex flow. Note that we plot v_r only for $t > 11$, ignoring the initial transient. The dashed curve in the figure represents the driving Reynolds number, $Re_1(t)$, which peaks at $\pm Re_{mod} = \pm 154.71$. We shall compare the values of $Re_1(t)$ to the horizontal line at $Re_1 = Re_{10}$ which, in the steady case, denotes the onset of Taylor vortex flow. The second horizontal line at $Re_1 = -Re_{10}$ corresponds to the onset of Taylor vortex flow of opposite polarity, which is created when the cylinder rotates in the opposite direction.

Initially the Reynolds number $Re_1(t)$ increases starting from the left of figure 1. Quasi-statically, we expect that, when $Re_1(t)$ reaches a value of the order of Re_{10}, azimuthal flow becomes unstable and v_r grows exponentially; then, as $Re_1(t)$ becomes smaller than Re_{10}, v_r peaks and quickly drops toward zero. The phase lag between the maximum values of $Re_1(t)$ and v_r is expected, as it takes a certain time for the fluid in the middle of the gap to respond to the drive. Soon afterward the motion of the inner cylinder becomes supercritical again but in the opposite direction, and a
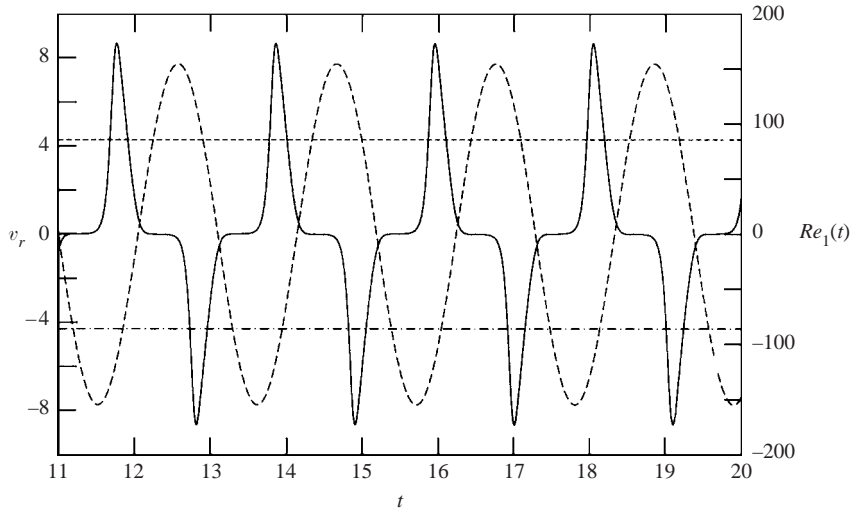
FIGURE 1. Radial velocity v_r versus time in the middle of the gap at the outflow computed at the (dimensionless) position $z = \pi/\alpha$, $r = (1 + \eta)/2(1 - \eta)$ for RTVF. $N = 12$, $K = 8$, $M = 4$, $\eta = 0.75$, $Re_{mod} = 154.71$ (which is $Re_{mod} = 1.1 Re_{mod,c}$ with $Re_{mod,c} = 140.65$), $\omega = 3$, $\alpha_c = 2.86$. Horizontal lines show $\pm Re_{10} = 85.78$ and the dashed curve is $Re_1(t)$.

new Taylor vortex pair is formed starting from the vanishingly small remains of the previous cycle. Note that this time the flow has opposite polarity, so v_r is negative (inflow jet). Examination of the flow at later times confirms that this pattern persists in a settled way, alternating Taylor vortex flow of opposite polarity. We call this flow reversing Taylor vortex flow (RTVF). For this flow the period of the driving $\tau = 2\pi/\omega$ is 2.09 and the flow responds to this driving with a period of 2.09, which is τ.

It is important to appreciate that the critical Reynolds number for the onset of reversing Taylor vortex flow is not $Re_{mod} = Re_{10}$ but higher. It is in fact possible that during the initial transient, v_r is of order unity, but, after a few cycles, Taylor vortex flow vanishes, and one observes a series of peaks of exponentially decreasing amplitude. The more striking feature of reversing Taylor vortex flow, the sharpness of the peaks, is due to the alternation of exponential growth and decay, and was also observed in the previous calculations of Barenghi & Jones (1989) and Kuhlmann *et al.* (1989) as well as in the experiments of G. Ahlers (1987, personal communication).

Figure 2 confirms that the observed change of sign of v_r at a particular position is significant, and that we are truly dealing with vortex pairs of opposite polarity. The arrows in this time sequence denote the radial and axial components of the velocity field. The height of each plot extends to one wavelength $2\pi/\alpha$, the (moving) inner cylinder is on the left and the (fixed) outer cylinder is on the right. At (*a*) we have a fully formed Taylor vortex pair in the forward direction, the outflow being at $z = \pi/\alpha$. At (*b*) we see the first appearance of reversed vortices close to the inner cylinder. At (*c*) and (*d*) the reversed Taylor vortex pair grows and extends across the gap. At (*e*) the forward Taylor vortex pair disappears, and at (*f*) we have a fully formed Taylor vortex pair in the reversed direction. Figure 2 thus shows a smooth transition from forward-rotation vortices to reverse-rotation vortices. Note that at stages (*c*) and (*d*) there are four cells within a wavelength. This situation is similar to the traditional case of (steady) counter-rotating Taylor vortex flow. The difference
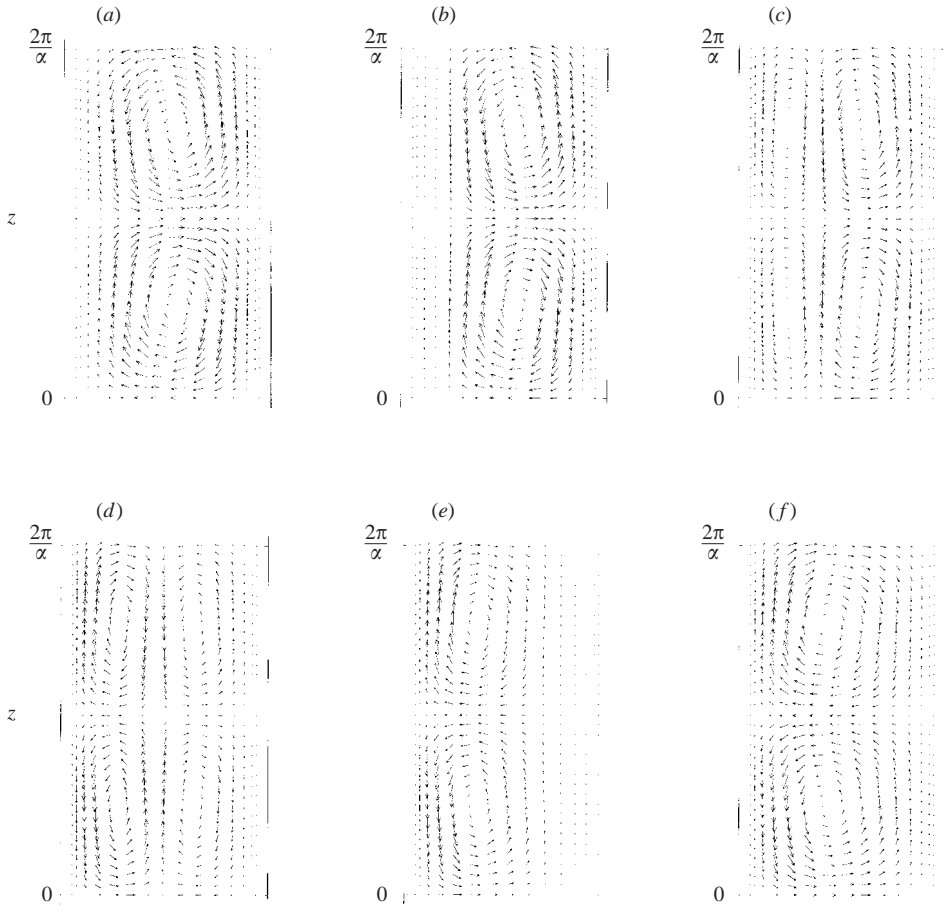
FIGURE 2. Reversing Taylor vortex flow at different times in the interval $12 \leqslant t \leqslant 12.5$. (*a*): Taylor vortex pair in the forward direction; note the outflow at $z = \pi/\alpha$; (*b*): reversing vortices appear near the inner cylinder; (*c*): the reversed Taylor vortices grow; (*d*): the reversed Taylor vortices fill the gap; (*e*): the forward Taylor vortex pair disappears; (*f*): fully formed Taylor vortex pair in the reverse direction.

is that in our (time-dependent) case the nodal line, which separates the reversed pair from the forward pair, moves across the gap during a cycle.

3.2. *Non-reversing Taylor vortex flow*

Figure 3 shows typical results at higher frequency of modulation. The parameters are now $Re_{mod} = 170.41$ and $\omega = 5$. It is apparent that the direction of the radial velocity, v_r, remains the same (the peaks are always positive), despite the change of direction of the driving inner cylinder. By examining plots similar to figure 2, we conclude that there is no sign of formation of a reversed vortex pair. We call this flow non-reversing Taylor vortex flow (NRTVF). In this case the period of the driving is $\tau = 1.26$ but the flow responds with a period of 0.63, which is $\tau/2$.

Many papers have reported the existence of synchronous and subharmonic solutions in the modulated Taylor–Couette problem, see for example, Barenghi (1991) and Kuhlmann *et al.* (1989). In the case of modulation of the outer cylinder around zero mean with a constantly rotating inner cylinder Lopez & Marques (2002) found
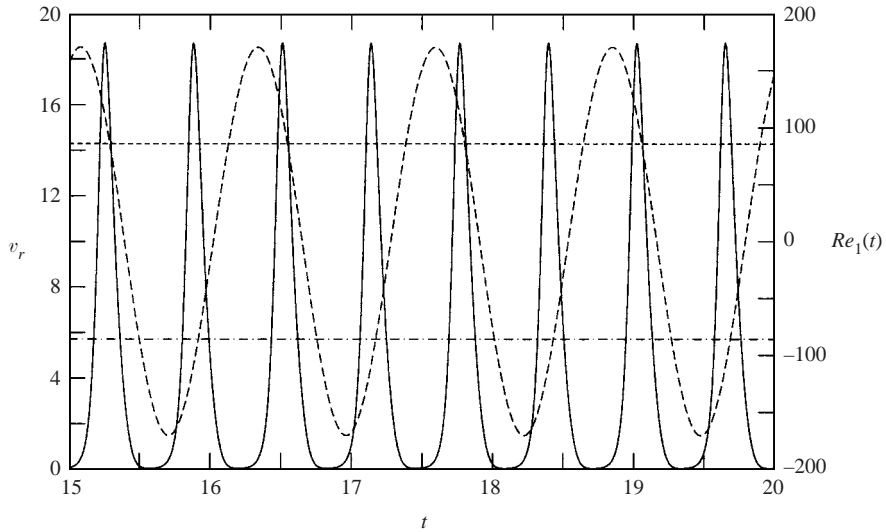
FIGURE 3. Radial velocity v_r versus time in the middle of the gap at the outflow computed again at the (dimensionless) position $z = \pi/\alpha$, $r = (1+\eta)/2(1-\eta)$ for NRTVF. Parameters as in figure 1 except $Re_{mod} = 170.41$ (which is $Re_{mod} = 1.1 Re_{mod,c}$ with $Re_{mod,c} = 154.91$), $\omega = 5$, $\alpha = 3.73$. Horizontal lines show $\pm Re_{10} = 85.78$ and the dashed curve is $Re_1(t)$.

that the synchronous solutions are non-reversing and the subharmonic solutions are reversing. In our problem we have found that both RTVF and NRTVF solutions are synchronous; to confirm it we calculated the radial velocity at the centre of the axial period, which is a symmetric position, and at various other non-symmetric points. We found that our solutions are indeed synchronous, with NRTVF being a harmonic of the imposed driving Reynolds number with frequency twice the driving frequency.

The two flows that we have found (RTVF and NRTVF) occur at different wavenumbers and figures 4 and 5 make the selection of the wavenumber clear. In figure 4 we see that α is always smaller for RTVF than NRTVF, and for both RTVF and NRTVF α decreases as ω increases. Figure 5 shows the stability boundaries in the (Re_{mod}, α)-plane for both RTVF and NRTVF at various values of the frequency ω. For each frequency there are two curves – one corresponding to RTVF and one corresponding to NRTVF – and each flow has its own critical wavenumber and critical Reynolds number. Whether the latter is higher or lower for RTVF than NRTVF (or vice versa) depends on ω.

Figure 6 shows how the Reynolds number Re_{mod} depends on frequency ω. Each point on the figure represents the result of a separate run of the code starting from initial seeding. The axial expansions $e^{i\alpha k z}$ contain multiples of the critical wavenumber shown in figure 4. It is apparent that at low frequencies RTVF is the first flow to onset but at higher frequencies NRTVF is the first. It is apparent from figure 5 that, if we increase the Reynolds number at a given frequency (say $\omega = 4$) holding the same value of wavenumber (say $\alpha = 3$), then circular Couette flow is followed by RTVF (say at $Re_{mod} \approx 152$) and then by NRTVF (say at $Re_{mod} \approx 178$). Note that even at the highest frequency of modulation of figure 6 ($\omega = 8$) the thickness of the Stokes layer is still comparable to the gap width ($\delta_s/\delta = 0.5$), so we are still far from the high-frequency limit studied, for example, by Hollerbach et al. (2002) in spherical geometry.
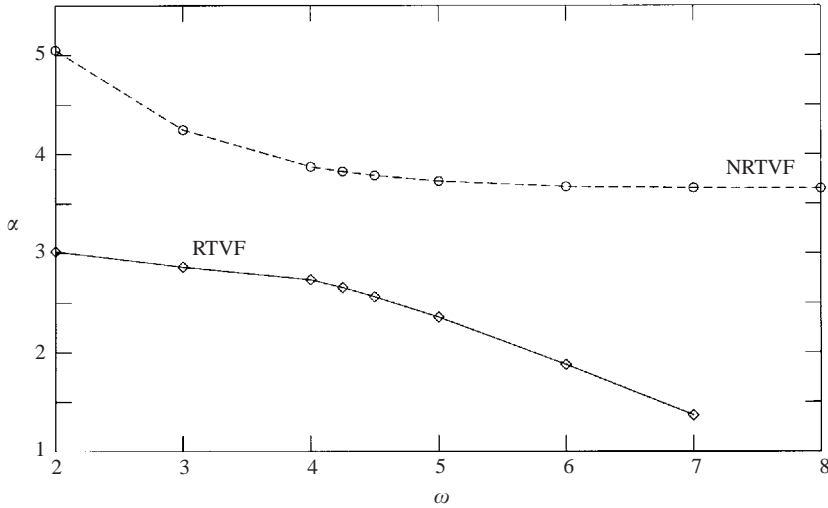
FIGURE 4. Critical wavenumber α of the inner cylinder versus frequency ω
for RTVF and NRTVF.
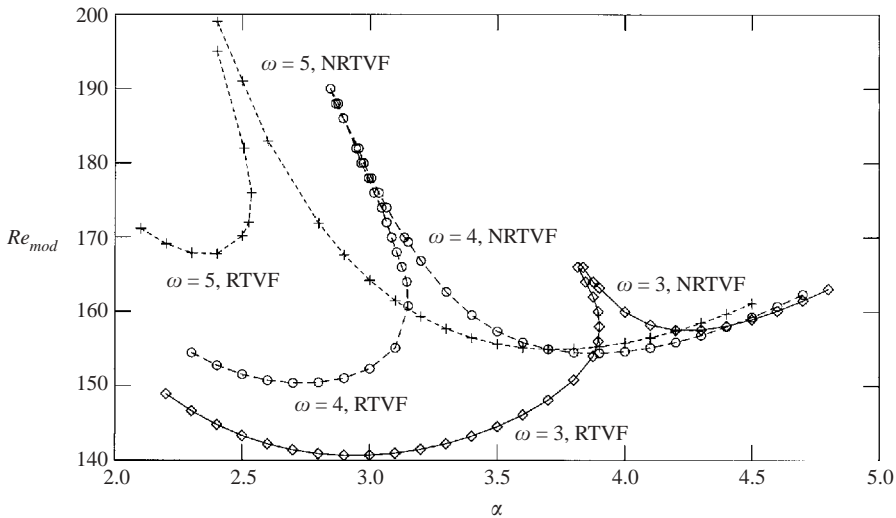
FIGURE 5. Modulation amplitude Re_{mod} of the inner cylinder versus wavenumber α
for RTVF and NRTVF at three frequencies.

Previous work on modulated Couette flow was done by Carmi & Tustaniwskyj (1981) who did not detect the existence of NRTVF. Their approach was based on studying the effects of infinitesimal perturbations over a cycle (Floquet theory). It is possible that NRTVF is due to finite-amplitude effects: whereas in RTVF v_r becomes negative for part of the cycle, NRTVF decays only to a certain order of magnitude level, at the end of a cycle, never becoming infinitesimal. For example, we found that $v_r \sim 10^{-1}$ for $\omega = 5$ and $Re_{mod} = 170.41$. However, non-reversing solutions have been found by Lopez & Marques (2002) using Floquet analysis for modulation of the outer cylinder, so NRTVF could be due to a linear instability too. Only a full Floquet
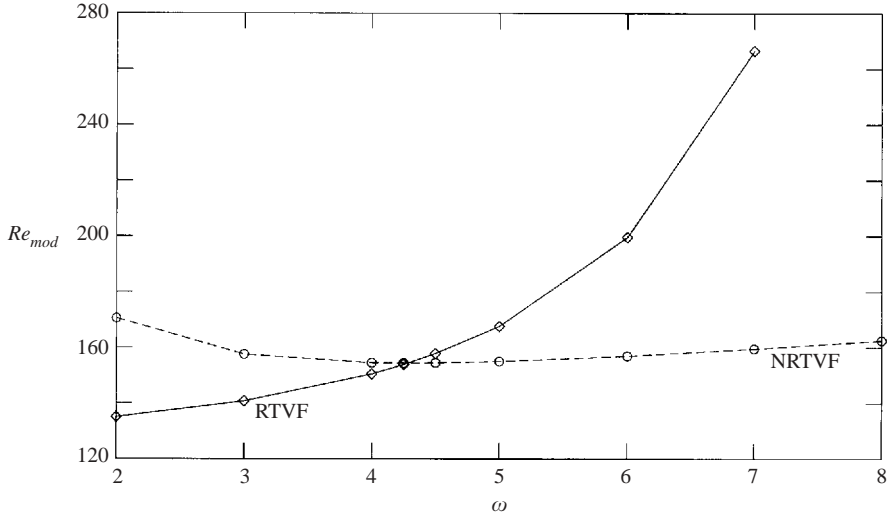
FIGURE 6. Critical Re_{mod} of the inner cylinder versus frequency ω for RTVF and NRTVF.
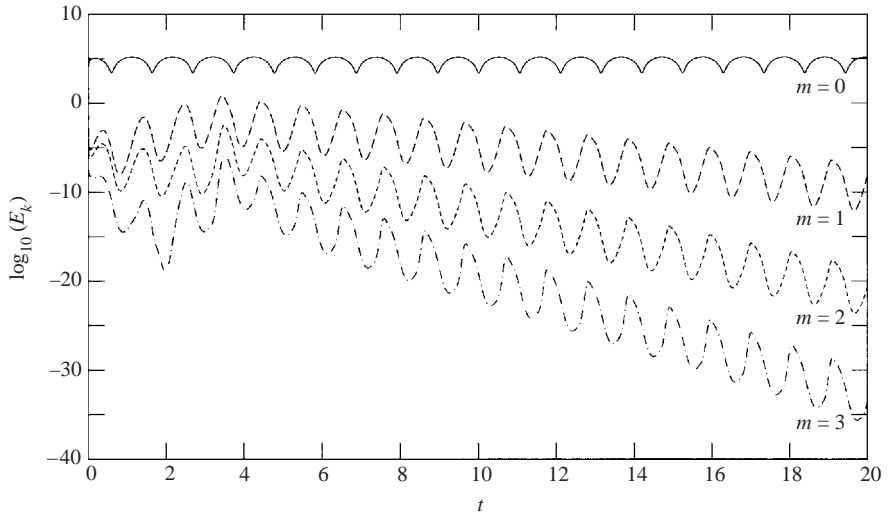
FIGURE 7. Logarithm of the kinetic energy (in arbitrary units as in Willis & Barenghi 2002) of the first azimuthal modes $m = 0, 1, 2, 3$ versus time for RTVF. Parameters as in figure 1.

analysis in the parameter range discussed can answer the question of whether the non-reversing solutions are due to finite-amplitude effects or not.

3.3. *Wavy modes*

All calculations were performed including a sufficient level of truncation so as to capture any possible three-dimensional nature of the flow. Azimuthal spectral truncations as high as $M = 8$ were used. In all cases the flow was always found to be axisymmetric.

Figures 7 and 8 show how the modes corresponding to $m \neq 0$ are initially seeded and grow, but, after the initial transient, they all eventually decay with time, leaving
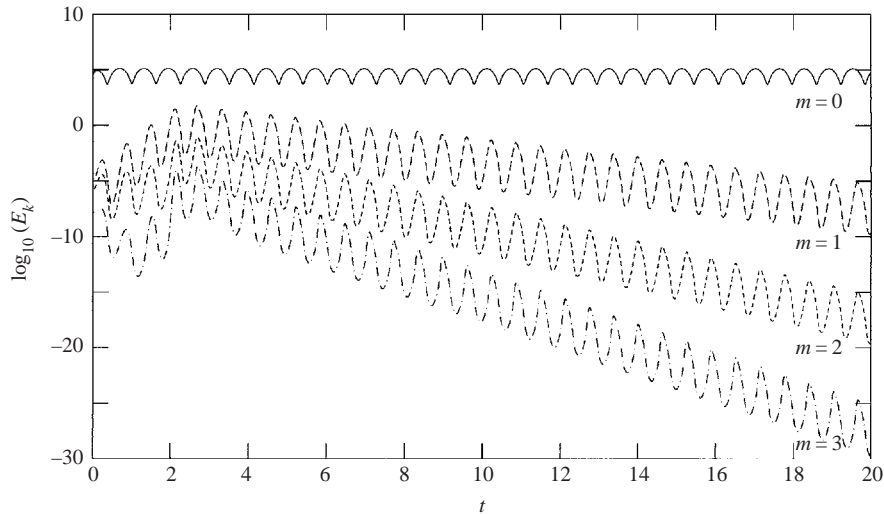
FIGURE 8. Logarithm of the kinetic energy (in arbitrary units as in Willis & Barenghi 2002) of the first azimuthal modes $m = 0, 1, 2, 3$ versus time for NRTVF. Parameters as in figure 3.

an axisymmetric, oscillatory flow ($m = 0$ only). This is in contrast to the results found for axial oscillations of the inner cylinder by Marques & Lopez (1997), and more recently for modulation of the outer cylinder by Lopez & Marques (2002), where the solutions are non-axisymmetric in some parameter regimes.

4. Conclusion

We have reconsidered the simplest case of time-modulated Taylor–Couette flow, in which the inner cylinder oscillates harmonically clockwise and counter-clockwise and the outer cylinder is held fixed. We have found that, if the amplitude of the modulation is large enough to destabilize circular Couette flow, two classes of Taylor vortex flow are possible: reversing and non-reversing. In the latter the Taylor vortex pairs always rotate in the same direction, despite the inner cylinder driving the flow in the opposite direction. NRTVF takes place at sufficiently high modulation frequencies for which there is not enough time for the toroidal motion to vanish to sufficiently small values (still these frequencies are small enough that δ_s is comparable to δ).

Further study of this problem should include a Floquet analysis of the flow to determine whether NRTVF is caused by linear instability (as in Lopez & Marques 2002) or finite-amplitude effects. If the latter is the case then NRTVF may be affected by the weak Ekman circulation (absent in our calculation) which is necessarily induced by the fixed top and bottom ends of the Taylor–Couette apparatus. The existence of Taylor vortices whose meridional circulation is not affected by the direction of the basic azimuthal flow is visible in some of the recent nonlinear numerical simulations of Zhang (2002) and Zhang & Zhang (2002) of time-modulated spherical Couette flow, so NRTVF is probably a robust effect which should be investigated experimentally. In cylindrical geometry it should be possible to control the Ekman circulation by using a non-uniform gap which produces a spatial ramp of the Reynolds number (as done by Ning, Ahlers & Cannell 1990 and Wiener *et al.* 1999 for example), so that the flow is subcritical near the top and bottom ends.

REFERENCES

BARENGHI, C. F. 1991 Computations of transitions and Taylor vortices in temporally modulated Taylor–Couette flow. *J. Comput. Phys.* **95**, 175–194.

BARENGHI, C. F. & JONES, C. A. 1989 Modulated Taylor–Couette flow. *J. Fluid Mech.* **208**, 127–160.

BARENGHI, C. F., PARK, K. & DONNELLY, R. J. 1980 Subharmonic destabilization of Taylor vortices near an oscillating cylinder. *Phys. Lett.* A **78**, 152–154.

BHATTACHARJEE, J. K., BANERJEE, K. & KUMAR, K. 1986 Modulated Taylor–Couette flow as a dynamical system. *J. Phys.* A: *Math. Gen.* **19**, L835–L839.

CARMI, S. & TUSTANIWSKYJ, J. I. 1981 Stability of modulated finite-gap cylindrical Couette flow: linear theory. *J. Fluid Mech.* **108**, 19–42.

DONNELLY, R. J. 1964 Experiments of the stability of viscous flows between rotating cylinders. III. Enhancement of stability by modulation. *Proc. R. Soc. Lond.* A **781**, 130–139.

HALL, P. 1983 On the nonlinear stability of slowly varying time-dependent viscous flows. *J. Fluid Mech.* **126**, 357–368.

HOLLERBACH, R., WIENER, R. J., SULLIVAN, I. S., DONNELLY. R. J. & BARENGHI, C. F. 2002 The flow around a torsionally oscillating sphere. *Phys. Fluids* **14**, 4192–4205.

HSIEH, D. Y. & CHEN, F. 1984 On a model study of Couette flow. *Phys. Fluids* **27**, 321–322.

KING, G. P., LE, Y., LEE, W., SWINNEY, H. L. & MARCUS, P. S. 1984 Wave speed in wavy Taylor-vortex flow. *J. Fluid Mech.* **141**, 365–390.

KUHLMANN, H., ROTH, D. & LUECKE, M. 1989 Taylor vortex flow under harmonic modulation of the driving. *Phys. Rev.* A **39**, 745–762.

JONES, C. A. 1985 Numerical methods for the transition to wavy Taylor vortices. *J. Comput. Phys.* **61**, 321–344.

LOPEZ, J. M. & MARQUES, F. 2001 Dynamics of three-tori in a periodically forced Navier–Stokes flow. *Phys. Rev. Lett.* **85**, 972–975.

LOPEZ, J. M. & MARQUES, F. 2002 Modulated Taylor–Couette flow: Onset of spiral modes. *Theor. Comput. Fluid Dyn.* **16**, 59–68

MARCUS, P. S. 1984 Simulation of Taylor vortex flow. Part 1. Numerical methods and comparison with experiment. *J. Fluid Mech.* **146**, 45–64.

MARQUES, F. & LOPEZ, J. M. 1997 Taylor–Couette flow with axial oscillations of the inner cylinder: Floquet analysis of the basic flow. *J. Fluid Mech.* **384**, 153–175.

NING, L., AHLERS, G. & CANNELL, D. S. 1990 Wave-number selection and travelling vortex waves in spatially ramped Taylor–Couette flow. *Phys. Rev. Lett.* **64**, 1235–1238.

RILEY, P. J. & LAWRENCE, R. L. 1977 Energy stability of modulated circular Couette flow. *J. Fluid Mech.* **79**, 535–552.

WALSH, T. J. & DONNELLY, R. J. 1988a Stability of modulated Couette flow. *Phys. Rev. Lett.* **58**, 2543–2546.

WALSH, T. J. & DONNELLY, R. J. 1988b Stability of modulated Couette flow. *Phys. Rev. Lett.* **60**, 700–703.

WIENER, R. J., DOLBY, D. C., GIBBS, G. C. & SQUIRES, B. 1999 Control of chaotic pattern dynamics in Taylor vortex flow. *Phys. Rev. Lett.* **83**, 2340–2343.

WILLIS, A. P. & BARENGHI, C. F. 2002 Hydromagnetic Taylor–Couette flow: numerical formulation and comparison with experiment. *J. Fluid Mech.* **463**, 361–375.

ZHANG, P. 2002 Simulations of nonlinear flows in spherical system. PhD thesis, Mathematics Department, University of Exeter.

ZHANG, P. & ZHANG, K. 2002 Vacillation in spherical Couette flow. *submitted*.